JACS
JOURNAL OF THE AMERICAN CHEMICAL SOCIETY
Article
pubs.acs.org/JACS

Two-Dimensional Cu_2Si Monolayer with Planar Hexacoordinate Copper and Silicon Bonding

Li-Ming Yang,*[,†] Vladimir Bačić,[‡] Ivan A. Popov,[§] Alexander I. Boldyrev,[§] Thomas Heine,[‡] Thomas Frauenheim,[†] and Eric Ganz[∥]

[†]Bremen Center for Computational Materials Science, University of Bremen, Am Falturm 1, 28359 Bremen, Germany
[‡]Engineering and Science, Jacobs University Bremen, Campus Ring 1, 28759 Bremen, Germany
[§]Department of Chemistry and Biochemistry, Utah State University, Logan, Utah 84322, United States;
[∥]Department of Physics, University of Minnesota, 116 Church St., SE, Minneapolis, Minnesota 55416, United States

Supporting Information

ABSTRACT: Two-dimensional (2D) materials with planar hypercoordinate motifs are extremely rare due to the difficulty in stabilizing the planar hypercoordinate configurations in extended systems. Furthermore, such exotic motifs are often unstable. We predict a novel Cu_2Si 2D monolayer featuring planar hexacoordinate copper and planar hexacoordinate silicon. This is a global minimum in 2D space which displays reduced dimensionality and rule-breaking chemical bonding. This system has been studied with density functional theory, including molecular dynamics simulations and electronic structure calculations. Bond order analysis and partitioning reveals 4c−2e σ bonds that stabilize the two-dimensional structure. We find that the system is quite stable during short annealing simulations up to 900 K, and predict that it is a nonmagnetic metal. This work opens up a new branch of hypercoordinate two-dimensional materials for study.

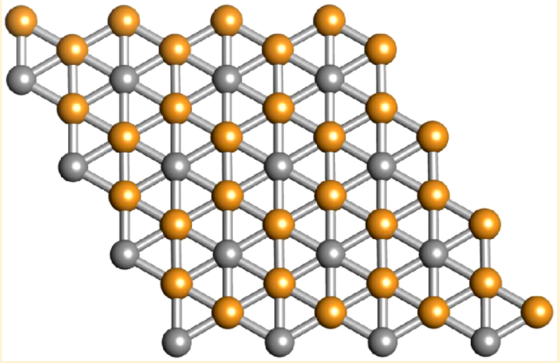

I. INTRODUCTION

Since the isolation and characterization of graphene,[1] the field of two-dimensional (2D) materials has attracted tremendous attention[2] and has evolved into a huge family of new exciting materials. This diverse group of 2D materials includes boron nitride,[3,4] dichalcogenide,[3,5] tertiary B−C−N,[6] and group IV,[7−11] II−VI,[12−14] and III−V[15−17] compounds. The ensuing impact on physics, materials science, and chemistry has been broad, including many fundamental and ingenious discoveries.

Considering these 2D materials from the viewpoint of structural and coordination chemistry, most have tricoordinated motifs, as demonstrated by graphene.[18] Only a few examples of (quasi)-planar tetracoordinated configurations have been reported; the first planar tetracoordinated carbon motifs in 2D networks based on C_5^{2-} were reported by Hoffmann et al.[19] followed by studies of B_xC_y,[20] SiC_2,[21] TiC,[22] and Al_xC.[23] Planar hexacoordinated motifs, first conceived by Schleyer and Exner in *isolated molecules*,[24] are extremely rare in 2D materials. Planar hexacoordinated 2D boron sheets have been proposed theoretically.[25−30] and boron nanoclusters have been observed spectroscopically.[31,32] It has been very challenging to create planar hypercoordinate 2D materials, as one needs to match the constituent elements both geometrically and electronically. In 2014, Schleyer and co-workers reviewed the history and progress in the prediction and fabrication of planar hypercoordinate molecules and extended systems.[33] In terms of fundamental science and potential applications, 2D hypercoordination materials are very exciting and attractive.

Recently, a Be_2C monolayer featuring quasi-planar hexacoordinate carbon (phC) has been proposed.[34] However, this material has a 0.46 Å vertical corrugation out of the plane. The theoretically predicted one-dimensional $-(SF_4-SF_4)_\infty-$ species with hexacoordinated sulfur atoms exhibiting direct S−S bonds await experimental confirmation.[35]

In this paper, on the basis of comprehensive density functional theory (DFT) computations, *we predict a new completely flat 2D hexacoordinated structure*. This is a 6-fold symmetric Cu_2Si monolayer with each Si atom coordinated with six Cu atoms to form a *planar hexacoordinate silicon* (phSi) structure. At the same time, each Cu is coordinated with three Si atoms and three Cu atoms to form a *planar hexacoordinate copper* (phCu) structure. These phSi and phCu elements are alternatively arranged to form an infinite sheet as shown in Figure 1a. This material is the first example of a simultaneously phSi and phCu-containing material. Our DFT computations demonstrate that this Cu_2Si monolayer has excellent stability. It is the global minimum structure in the 2D space, and so has promise for experimental synthesis.

Received: December 28, 2014
Published: February 2, 2015

DOI: 10.1021/ja513209c
J. Am. Chem. Soc. 2015, 137, 2757−2762

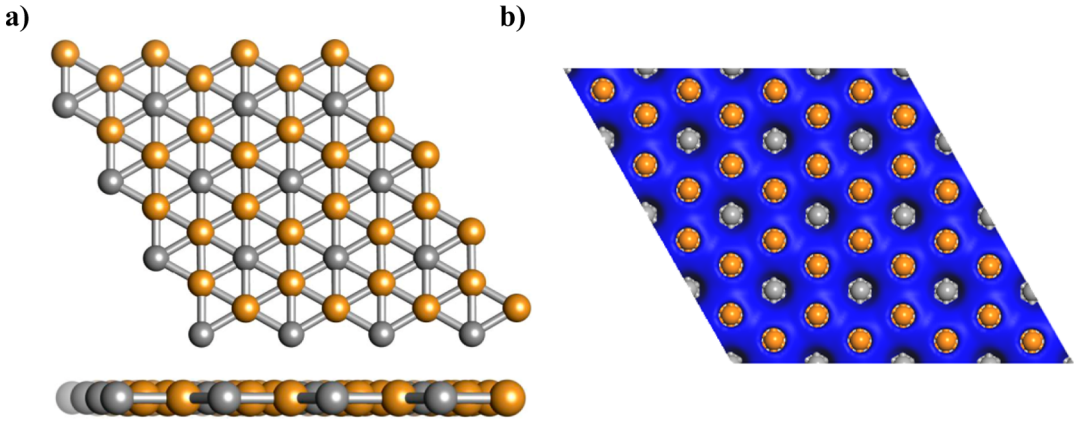

Figure 1. (a) Top and side views of the ball and stick model of the 2D Cu_2Si monolayer. 4 × 4 section of extended monolayer. Note that bonds to atoms outside section exist, but are not shown. (b) Deformation charge density of the 2D Cu_2Si monolayer. Blue refers to electron accumulation. Copper atoms are brown, and silicon gray.

II. COMPUTATIONAL METHODOLOGIES

The electronic structure and total energy were calculated using DFT via the plane-wave pseudopotential (PWPP) technique implemented in the Vienna *ab initio* simulation package (VASP).[36] The projector-augmented wave (PAW)[37,38] method was used to represent the ion−electron interaction. The generalized gradient approximation (GGA) expressed by the PBE functional,[39] and a 500 eV cutoff for the plane-wave basis set were adopted in all calculations. The convergence threshold was set as 10^{-6} eV in energy and 10^{-3} eV/Å in force. We placed the monolayer Cu_2Si sheet in the *xy* plane with the *z* direction perpendicular to the layer plane. A vacuum space of 15 Å in the *z* direction was used to avoid interactions between adjacent layers. The Brillouin zone was sampled with a 12 × 12 × 1 Γ-centered Monkhorst−Pack (MP)[40] K-points grid. Phonon dispersion was calculated using density-functional perturbation theory (DFPT),[41] as implemented in the Quantum-ESPRESSO package.[42] This was done within the local-density approximation (LDA) and using PAW pseudopotentials. Cutoffs of 80 and 1000 Ry were used for wave functions and charge density, respectively. The Brillouin zone was sampled with a 32 × 32 × 1 Monkhorst−Pack (MP) grid, and dynamical matrices were calculated on a 12 × 12 × 1 MP grid. For the deformation charge density, the electronic configuration used for Cu is $3d^{10}4s^1$ and for Si is $3s^23p^2$.

Born−Oppenheimer molecular dynamics (BOMD) simulations were performed to assess the thermal stability of the Cu_2Si monolayer. The DSPP pseudopotential and GGA PBE functional were used, as implemented in Dmol^3 software[43,44] in Materials Studio 7.0. MD simulations in the NVT ensemble were carried out for 3−10 ps with a time step of 1.0 fs (parameters: accuracy fine, DND, DFT-D TS, SCF = 2×10^{-6}, smearing = 0.01, DIIS = 10, Nose-Hoover, Nose Q = 2, Nose chain length = 2). Due to limitations of the program, no warm-up period was used. For the MD simulations, a 4 × 4 supercell was used in a 12.5 × 16.5 × 12 Å^3 box. The temperature was controlled using the Nosé−Hoover method.[45] Materials studio was also used to create the initial structures and visualize the results.

The crystal structure predictions were performed with particle-swarm optimization (PSO) method as implemented in the CALYPSO code.[46] The PSO algorithm offers an efficient and fast way to obtain reliable structures with only the input of chemical composition. The algorithm searches for structures with space group symmetry.

In our PSO simulation, the population size and the number of generation were set to be 30. The number of formula units per simulation cell was set as 1 to 6; that is, unit cells containing total number atoms of 3, 6, 9, 12, 15, and 18 were considered. The structure relaxations during the PSO simulation were performed using the PBE functional as implemented in VASP. High-quality renderings of the molecular structures were produced with the UCSF Chimera package.[47]

The same parameters were used for the periodic NBO and SSAdNDP calculations as for the VASP calculations. Similar to standard NBO code,[48−50] periodic NBO allows determination of Lewis elements of localized bonding, such as 1c−2e bonds (lone pairs) and 2c−2e bonds (classical two-center two-electron bonds), whereas SSAdNDP enables delocalized bonding (nc-2e bonds, $n > 2$) to be found in addition. The SSAdNDP projection algorithm was used to obtain a representation of the delocalized plane wave DFT results in a localized atomic orbital basis. As long as an appropriate atomic orbital basis set is chosen (it is usually trimmed of any functions with angular momentum $l \geq 4$ as well as diffuse functions with exponents <0.1), projection is found to result in an accurate density matrix. For the 2D Cu_2Si system, the Def2-SV(P) basis set was used to represent the projected PW density using a 7 × 7 × 3 k-point grid. This basis set was selected so that on average less than 1% of the density of each occupied plane wave band was lost in projecting into the AO basis to guarantee that the density matrix used in the SSAdNDP procedure accurately represents the original plane wave results. The Visualization for Electronic and Structural Analysis software (VESTA, series 3)[51] was used for visualization of the SSAdNDP results.

III. RESULTS AND DISCUSSION

The ground state structure of Cu_2Si was obtained using a comprehensive particle swarm structural search with CALYPSO code[46] followed by the full relaxation of random structures with VASP[36] (see details in section II). Having located the global minimum structure of the Cu_2Si monolayer (Figure 1a), we then performed an analysis of properties including chemical bonding, cohesive energy, mechanical properties, dynamic stability, thermal stability, and electronic properties.

To evaluate the chemical bonding of the phSi and phCu atoms, we computed the deformation electronic density. This quantity is defined as the total electronic density of the Cu_2Si monolayer minus the electron density of isolated Cu and Si atoms at their respective positions. Thus, the deformation density is well suited to probe the valence electron delocalization. Computational details are given in the Supporting Information. Indeed, Figure 1b shows a smooth, delocalized electron deformation density, as one would expect for a metal, with holes in the deformation electron density near the atomic positions (due to the pseudopotentials). The Hirshfeld charge analysis (from Dmol^3 calculations) shows that each Cu atom transfers 0.06 e to each Si atom.

To understand the unique chemical bonding in Cu_2Si monolayer, we have utilized periodic natural bond orbital (NBO)[52] analysis. In total, there are 22 valence electrons from

DOI: 10.1021/ja513209c
J. Am. Chem. Soc. 2015, 137, 2757−2762

two Cu atoms and four valence electrons from each Si atom per unit cell. This analysis found ten *d*-type lone pairs on the two Cu atoms (five on each atom) with occupation number of 1.9–2.0 |e| (see Figure 2).

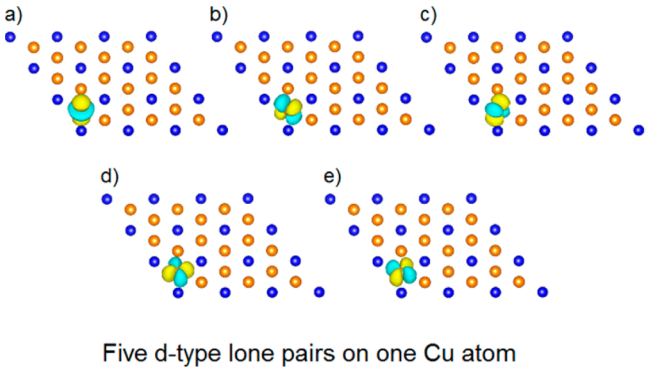

Figure 2. Bonding structure of the Cu_2Si monolayer. Five *d*-type lone pairs on one Cu atom.

We have also used an extension of the periodic natural bond orbital method, the Solid State Adaptive Natural Density Partitioning (SSAdNDP)[53] method. It is noteworthy that both methods have shown the absence of any classical two-center two-electron (2c–2e) σ bonds. The SSAdNDP analysis identifies both localized (nc–2e bonds, $n \leq 2$) and delocalized (nc–2e bonds, $n > 2$) bonding elements in the Cu_2Si monolayer. It found the same 10 lone pairs on two Cu atoms with occupation number 1.9–2.0 |e| as well as three 4c–2e σ bonds with occupation number 1.9 |e|, thus accounting for 26 electrons per unit cell. These 4c–2e σ bonds are shown in Figure 3a–c. Thus, one can see that *the delocalized bonding*

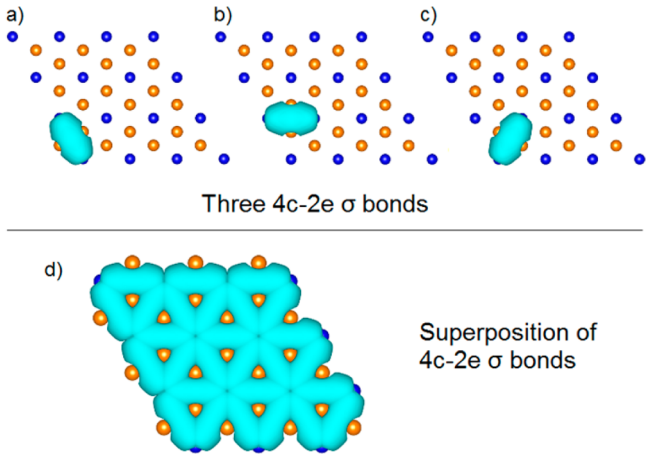

Figure 3. Bonding structure of the Cu_2Si monolayer. (a–c) Individual 4c–2e σ bonds. (d) superposition of 4c–2e σ bonds. Copper is orange, and silicon is blue.

governs the planar geometry of the Cu_2Si sheet. This chemical bonding picture is consistent with the symmetry of the 2D crystal. We observe that the deformation charge density of Figure 1b is similar to the superposition of 4c–2e σ bonds shown in Figure 3d.

The calculated Si–Cu and Cu–Cu bond lengths are both close to 2.38 Å. One unit cell of the Cu_2Si monolayer consists of two Cu atoms and one Si atom, with optimized lattice constants of $a = b = 4.123$ Å. The band structure indicates the material is metallic with a large density-of-states (DOS) at the Fermi level. The Cu_2Si monolayer is diamagnetic as confirmed by a spin-polarized computation, indicating that the compound has a nonmagnetic ground state and there are no unpaired electrons or unsaturated dangling bonds.

To evaluate the stability of this structure, we first computed the cohesive energy $E_{coh} = (xE_{Si} + 2xE_{Cu} - xE_{Cu2Si})/3x$, with E_{Cu}, E_{Si}, and E_{Cu2Si} being the total energies of a single Cu atom, a single Si atom, and one unit cell of the Cu_2Si monolayer. The Cu_2Si monolayer has a cohesive energy of 3.46 eV/atom. For comparison, using the same computational method, the cohesive energies of graphene, silicene, and germanene are 7.85, 3.98, and 3.26 eV/atom, respectively. Thus, while the cohesive energy is significantly lower than that of the Cu and Si 3D bulk phases, it is sufficient when restricting the material to 2D, indicated by the stronger binding energy compared to germanene, and comparable to that of silicene.

The mechanical properties are important for potential application of the Cu_2Si material. The in-plane Young modulus, (or in-plane stiffness), is commonly used to evaluate the mechanical stability of 2D layered materials. We compare the calculated value of our new material to reported experimental values[54] and previous theoretical results[55,56] for several commonly known 2D materials, including graphene, MoS_2, germanene, and silicene. For the Cu_2Si monolayer, the in-plane stiffness was computed to be 93 N/m, which is lower than that of graphene (295 N/m). However, it is comparable to the in-plane stiffness of the MoS_2 monolayer (124 N/m), and higher than germanene (42 N/m) and silicene (61 N/m) computed at the same theoretical levels. Thus, the Cu_2Si monolayer shows strong mechanical stability.

The dynamical stability of the Cu_2Si monolayer was tested by calculating the phonon dispersion along the high-symmetry lines (Figure 4). All the frequencies are real, indicating its

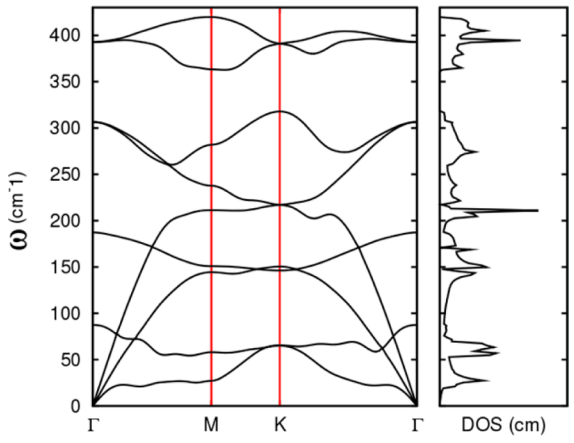

Figure 4. Phonon dispersion and phonon density of states of the monolayer Cu_2Si sheet. Γ (0, 0, 0), M (0, 1/2, 0), and K (1/3, 2/3, 0) refer to special points in the first Brillouin zone in reciprocal space.

kinetic stability. No imaginary phonon modes are found in the whole Brillouin zone. In particular, the highest frequency reaches up to 420 cm^{-1}, indicating robust Cu–Si interaction. The lowest optical mode (90 cm^{-1}) corresponds to out-of-plane vibration of Cu atoms, while the highest, doubly degenerate, optical mode (390 cm^{-1}) corresponds to in-plane vibrations of Cu and Si atoms.

DOI: 10.1021/ja513209c
J. Am. Chem. Soc. 2015, 137, 2757–2762

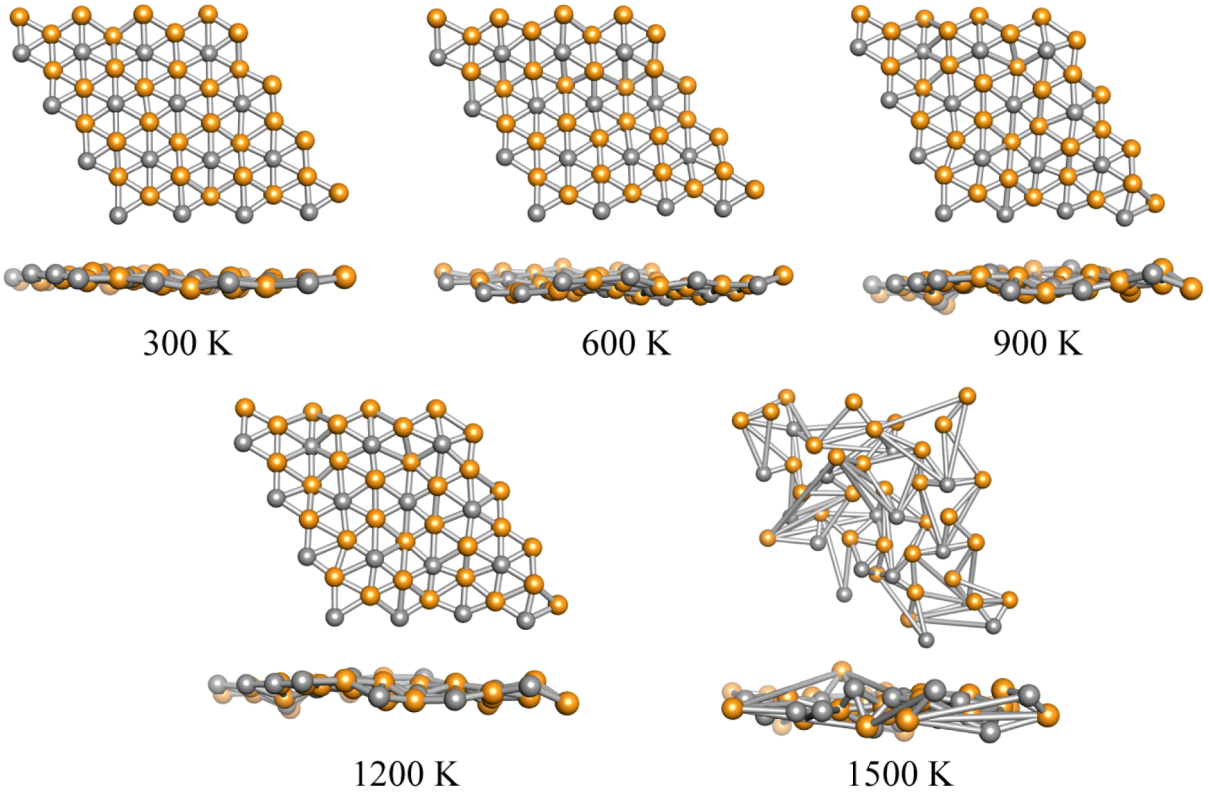

Figure 5. Snapshots of the final frame of each molecular dynamics simulation from 300 to 1500 K (top and side views). Bonds to atoms outside this 4 × 4 section exist but are not shown.

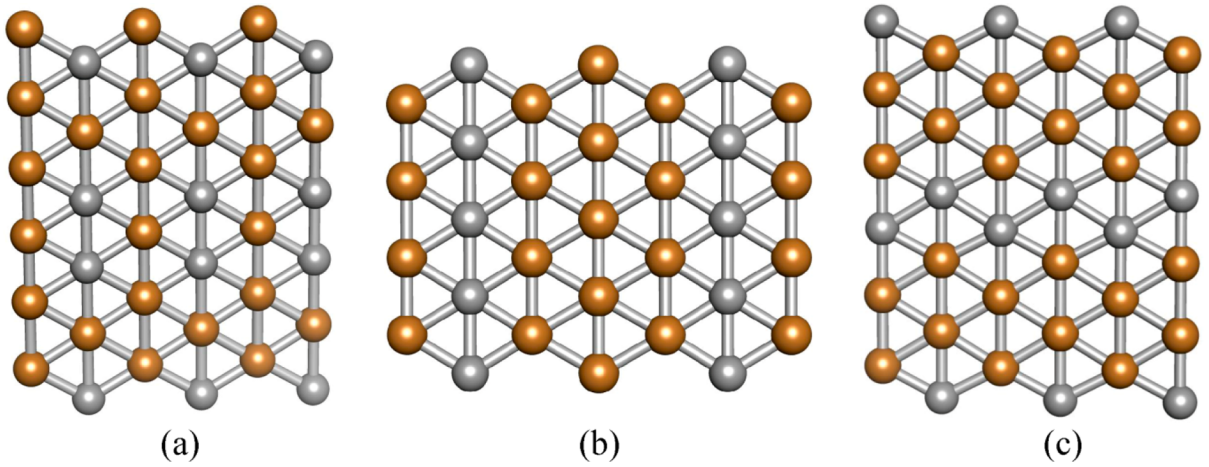

Figure 6. Low lying isomers found by particle swarm search. Copper atoms are brown, and silicon is gray. Bonds to atoms outside of these sections exist but are not shown.

To verify that this new material will be stable at ambient conditions, we have performed Born−Oppenheimer molecular dynamics simulations. A 4 × 4 supercell was used in the MD simulations. A series of individual MD simulations were carried out to evaluate the thermal stability of the monolayer Cu_2Si material at temperatures of 300, 600, 900, 1200, and 1500 K (of duration 3, 4, 10, 10, and 4 ps respectively). Snapshots taken at the end of each simulation are shown in Figure 5 and also from a different perspective in the Supporting Information (SI). From the snapshots, one can see that the planar hexacoordinate motifs were generally well-kept. The structure survives a 10 ps anneal up to 900 K. A survey of bond lengths shows individual bond lengths increasing temporarily by up to 16% at 900 K in the last 1 ps of the simulation, although most bonds stay shorter most of the time. Looking at the final 900 K snapshot in Figure 5 and in the SI, the system is still holding together well. At 1200 K, by 10 ps, the system is clearly starting to melt. The atoms are fluctuating significantly, and a survey of bond lengths shows individual bond lengths increasing temporarily by up to 37% at 1200 K. At 1500 K, the structure is seriously disrupted already after only 4 ps, and atoms have already started to exchange positions. The above results reveal that the Cu_2Si monolayer has very good thermal stability and can maintain its structural integrity during brief annealing up to 900 K.

After confirming that Cu_2Si monolayer is a stable local minimum structure, we show that this monolayer is actually a

DOI: 10.1021/ja513209c
J. Am. Chem. Soc. 2015, 137, 2757−2762

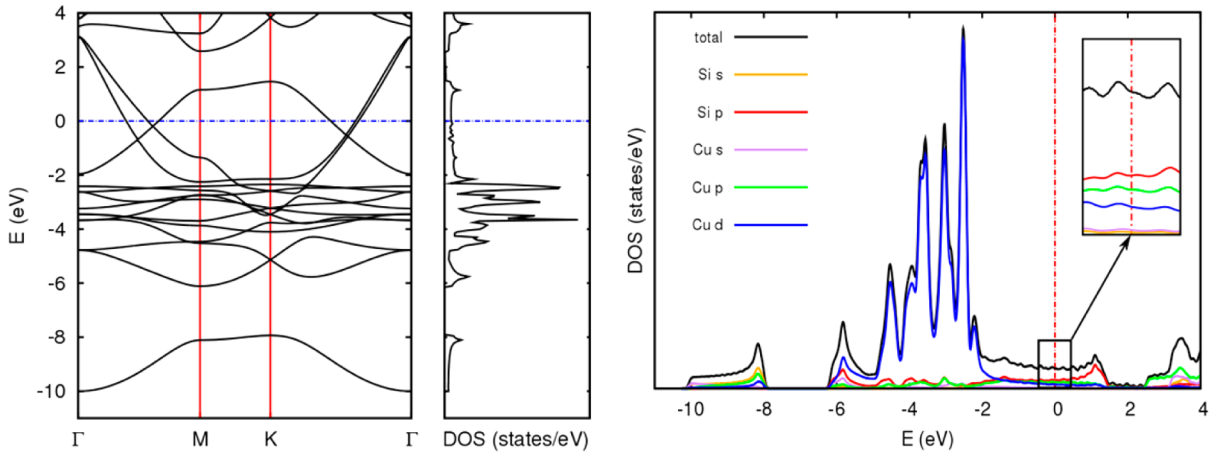

Figure 7. Electronic structure of Cu_2Si monolayer: band structure (left), total density of states (DOS) (middle), and projected density of states (PDOS) (right). The Fermi level is at 0 eV.

global minimum in 2D space. To address this issue, we have performed a global minimum search for the lowest-energy structure for Cu_2Si in the 2D space using first-principles based particle swarm optimization.[46] After a comprehensive structural search, the hexacoordinate Cu_2Si layer discussed above with uniform and highly symmetrical distribution of Si and Cu atoms was found to be the lowest energy structure in the 2D space. The three lowest stable planar hexacoordinate structures for 2D Cu_2Si with different patterns and relative distributions of Cu and Si atoms in the plane are shown in Figure 6. These three structures are low-lying isomers featuring planar hexacoordinate configurations with relative energies of 80, 121, and 160 meV/atom, respectively.

As a result of the search, we also found some planar tetracoordinate motifs for the Cu_2Si sheet. These structures also have very interesting structural properties: each Si atom binds to four Cu atoms in the same plane to form a ptSi moiety. However, their total energies are significantly higher than those of the four planar hexacoordinate motifs.

We have also considered buckled structures of 2D Cu_2Si, though all of them were found to be higher in energy than the planar hexacoordinate motifs. Therefore, the phSi/phCu-containing Cu_2Si monolayer is the global minimum structure in the 2D space. This result is very exciting because the Cu_2Si monolayer is the first extended planar hexacoordinate Si-containing structure. Previously, phSi motifs have only been rarely predicted computationally in isolated molecules such as $SiCu_6H_6$[57] and $SiB_4Si_2^-$.[58] We do not know whether these two molecules are global minima, and there has not been any follow-up experimental confirmation. Moreover, Cu atoms in the Cu_2Si monolayer are also in a planar hexacoordinate configuration. To our knowledge, there is no report to date of planar hexacoordinate Cu motifs, either on isolated molecules or in periodic structures. Since the phSi/phCu-containing Cu_2Si monolayer is the global minimum structure in 2D space, it holds great potential to be realized experimentally.

To get insight into electronic properties, we have computed the band structure as well as its density of states (DOS). As shown in Figure 7, the material shows a band structure typical for metals. The metallic character of Cu_2Si is demonstrated by the Fermi level ($E = 0$) being located inside the bands, and no observation of a band gap at this energy. Therefore, unlike semimetallic graphene, the Cu_2Si monolayer is a diamagnetic metal.

The projected density of states (PDOS) analysis shows that below the Fermi energy the major contribution comes from Cu 3*d*-states. The states at the Fermi level are dominated by the Si-3*p*, Cu-4*p* and Cu-3*d* states, with Si-3*p* more pronounced than Cu-4*p* and -3*d*. There is apparent hybridization between Si 3*p*- and Cu 4*p*-, 3*d*-states. This is consistent with the chemical bonding analysis of the Cu_2Si monolayer.

IV. CONCLUSIONS

In summary, we have designed a new stable planar *hexacoordinate* 2D Cu_2Si monolayer. This material is metallic. In the Cu_2Si monolayer, each Si atom is coordinated to six Cu atoms to form a phSi moiety. Furthermore, each Cu atom is coordinated to three Cu and three Si atoms to form a phCu configuration. Chemical bonding analysis shows that multicenter σ bonds stabilize the two-dimensional structure. The Cu_2Si monolayer has strong chemical bonding and high in-plane stiffness. Local structural stability is predicted by the absence of any imaginary phonon modes. Molecular dynamics simulations show that this material is stable during short annealing runs up to 900 K. A Particle Swarm search confirmed that the Cu_2Si monolayer is the global minimum structure in 2D space. Considering the rapid development of experimental techniques for fabrication of low-dimensional materials in recent years, we are optimistic that the Cu_2Si monolayer can be fabricated experimentally in the near future.

■ ASSOCIATED CONTENT

Supporting Information

Complete ref 42, and snapshots (angle view) from the final state of each of the molecular dynamics simulations from 300 to 1500 K. This material is available free of charge via the Internet at http://pubs.acs.org.

■ AUTHOR INFORMATION

Corresponding Author

*lmyang.uio@gmail.com

Notes

The authors declare no competing financial interest.

■ ACKNOWLEDGMENTS

Support in Germany by Fellowship of Hanse-Wissenschafts-Kolleg (HWK) (Institute for Advanced Study) and Research

DOI: 10.1021/ja513209c
J. Am. Chem. Soc. 2015, 137, 2757−2762

Scholarship of University of Bremen (to L.-M.Y), Deutsche Forschungsgemeinschaft, HE 3543/18-1), The European Commission (FP7-PEOPLE-2009-IAPP QUASINANO, GA 251149 and FP7-PEOPLE-2012-ITN MoWSeS, GA 317451), and in the United States by the National Science Foundation (CHE-1361413 to A.I.B.) are gratefully acknowledged. L.-M.Y and E.G. thank Matthew Dornfeld for his assistance. We thank the Minnesota supercomputer Institute, HLRN & JUROPA supercomputers for support. Computer, storage, and other resources from the Division of Research Computing in the Office of Research and Graduate Studies at Utah State University are gratefully acknowledged. This work is dedicated to the memory of Professor Paul von Ragué Schleyer.

REFERENCES

(1) Novoselov, K. S.; Geim, A. K.; Morozov, S. V.; Jiang, D.; Zhang, Y.; Dubonos, S. V.; Grigorieva, I. V.; Firsov, A. A. *Science* **2004**, *306*, 666.
(2) Miro, P.; Audiffred, M.; Heine, T. *Chem. Soc. Rev.* **2014**, *43*, 6537.
(3) Novoselov, K. S.; Jiang, D.; Schedin, F.; Booth, T. J.; Khotkevich, V. V.; Morozov, S. V.; Geim, A. K. *Proc. Natl. Acad. Sci. U. S. A.* **2005**, *102*, 10451.
(4) Jin, C.; Lin, F.; Suenaga, K.; Iijima, S. *Phys. Rev. Lett.* **2009**, *102*, 195505.
(5) Joensen, P.; Frindt, R. F.; Morrison, S. R. *Mater. Res. Bull.* **1986**, *21*, 457.
(6) Ci, L.; Song, L.; Jin, C.; Jariwala, D.; Wu, D.; Li, Y.; Srivastava, A.; Wang, Z. F.; Storr, K.; Balicas, L.; Liu, F.; Ajayan, P. M. *Nat. Mater.* **2010**, *9*, 430.
(7) Cahangirov, S.; Topsakal, M.; Aktürk, E.; Şahin, H.; Ciraci, S. *Phys. Rev. Lett.* **2009**, *102*, 236804.
(8) De Padova, P.; Quaresima, C.; Ottaviani, C.; Sheverdyaeva, P. M.; Moras, P.; Carbone, C.; Topwal, D.; Olivieri, B.; Kara, A.; Oughaddou, H.; Aufray, B.; Le Lay, G. *Appl. Phys. Lett.* **2010**, *96*, 261905.
(9) Feng, B.; Ding, Z.; Meng, S.; Yao, Y.; He, X.; Cheng, P.; Chen, L.; Wu, K. *Nano Lett.* **2012**, *12*, 3507.
(10) Miyamoto, Y.; Yu, B. D. *Appl. Phys. Lett.* **2002**, *80*, 586.
(11) Cahangirov, S.; Audiffred, M.; Tang, P.; Iacomino, A.; Duan, W.; Merino, G.; Rubio, A. *Phys. Rev. B* **2013**, *88*, 035432.
(12) Wu, W.; Lu, P.; Zhang, Z.; Guo, W. *ACS Appl. Mater. Interfaces* **2011**, *3*, 4787.
(13) Botello-Méndez, A. R.; López-Urías, F.; Terrones, M.; Terrones, H. *Nano Lett.* **2008**, *8*, 1562.
(14) Topsakal, M.; Cahangirov, S.; Bekaroglu, E.; Ciraci, S. *Phys. Rev. B* **2009**, *80*, 235119.
(15) Du, A. J.; Zhu, Z. H.; Chen, Y.; Lu, G. Q.; Smith, S. C. *Chem. Phys. Lett.* **2009**, *469*, 183.
(16) Şahin, H.; Cahangirov, S.; Topsakal, M.; Bekaroglu, E.; Akturk, E.; Senger, R. T.; Ciraci, S. *Phys. Rev. B* **2009**, *80*, 155453.
(17) Li, H.; Dai, J.; Li, J.; Zhang, S.; Zhou, J.; Zhang, L.; Chu, W.; Chen, D.; Zhao, H.; Yang, J.; Wu, Z. *J. Phys. Chem. C* **2010**, *114*, 11390.
(18) Xu, M.; Liang, T.; Shi, M.; Chen, H. *Chem. Rev.* **2013**, *113*, 3766.
(19) Pancharatna, P. D.; Mendez-Rojas, M. A.; Merino, G.; Vela, A.; Hoffmann, R. *J. Am. Chem. Soc.* **2004**, *126*, 15309.
(20) Luo, X.; Yang, J.; Liu, H.; Wu, X.; Wang, Y.; Ma, Y.; Wei, S.-H.; Gong, X.; Xiang, H. *J. Am. Chem. Soc.* **2011**, *133*, 16285.
(21) Li, Y.; Li, F.; Zhou, Z.; Chen, Z. *J. Am. Chem. Soc.* **2011**, *133*, 900.
(22) Zhang, Z. H.; Liu, X. F.; Yakobson, B. I.; Guo, W. L. *J. Am. Chem. Soc.* **2012**, *134*, 19326.
(23) Dai, J.; Wu, X.; Yang, J.; Zeng, X. C. *J. Phys. Chem. Lett.* **2014**, *5*, 2058.
(24) Exner, K.; Schleyer, P. v. R. *Science* **2000**, *290*, 1937.
(25) Tang, H.; Ismail-Beigi, S. *Phys. Rev. Lett.* **2007**, *99*, 115501.
(26) Yang, X.; Ding, Y.; Ni, J. *Phys. Rev. B* **2008**, *77*, 041402.
(27) Liu, Y.; Penev, E. S.; Yakobson, B. I. *Angew. Chem., Int. Ed.* **2013**, *52*, 3156.
(28) Liu, H.; Gao, J.; Zhao, J. *Sci. Rep.* **2013**, *3*, 3238.
(29) Wu, X.; Dai, J.; Zhao, Y.; Zhuo, Z.; Yang, J.; Zeng, X. C. *ACS Nano* **2012**, *6*, 7443.
(30) Penev, E. S.; Bhowmick, S.; Sadrzadeh, A.; Yakobson, B. I. *Nano Lett.* **2012**, *12*, 2441.
(31) Piazza, Z. A.; Hu, H.-S.; Li, W.-L.; Zhao, Y.-F.; Li, J.; Wang, L.-S. *Nat. Commun.* **2014**, *5*, 3113.
(32) Li, W.-L.; Chen, Q.; Tian, W.-J.; Bai, H.; Zhao, Y.-F.; Hu, H.-S.; Li, J.; Zhai, H.-J.; Li, S.-D.; Wang, L.-S. *J. Am. Chem. Soc.* **2014**, *136*, 12257.
(33) Yang, L.-M.; Ganz, E.; Chen, Z.; Wang, Z.-X.; Schleyer, P. v. R. *Angew. Chem.* **2014**, DOI: 10.1002/anie.201410407 and 10.1002/ange.201410407.
(34) Li, Y.; Liao, Y.; Chen, Z. *Angew. Chem., Int. Ed.* **2014**, *53*, 7248.
(35) Popov, I. A.; Averkiev, B. B.; Starikova, A. A.; Boldyrev, A. I.; Minyaev, R. M.; Minkin, V. I. *Angew. Chem., Int. Ed.* **2015**, *54*, 1476.
(36) Kresse, G.; Hafner, J. *Phys. Rev. B* **1993**, *47*, 558.
(37) Blöchl, P. *Phys. Rev. B* **1994**, *50*, 17953.
(38) Kresse, G.; Joubert, D. *Phys. Rev. B* **1999**, *59*, 1758.
(39) Perdew, J. P.; Burke, K.; Ernzerhof, M. *Phys. Rev. Lett.* **1996**, *77*, 3865.
(40) Monkhorst, H. J.; Pack, J. D. *Phys. Rev. B* **1976**, *13*, 5188.
(41) Baroni, S.; de Gironcoli, S.; Dal Corso, A.; Giannozzi, P. *Rev. Mod. Phys.* **2001**, *73*, 515.
(42) Paolo, G.; et al. *J. Phys.: Condens. Matter* **2009**, *21*, 395502.
(43) Delley, B. *J. Chem. Phys.* **1990**, *92*, 508.
(44) Delley, B. *J. Chem. Phys.* **2000**, *113*, 7756.
(45) Martyna, G. J.; Klein, M. L.; Tuckerman, M. *J. Chem. Phys.* **1992**, *97*, 2635.
(46) Wang, Y.; Lv, J.; Zhu, L.; Ma, Y. *Phys. Rev. B* **2010**, *82*, 094116.
(47) Pettersen, E. F.; Goddard, T. D.; Huang, C. C.; Couch, G. S.; Greenblatt, D. M.; Meng, E. C.; Ferrin, T. E. *J. Comput. Chem.* **2004**, *25*, 1605.
(48) Reed, A. E.; Curtiss, L. A.; Weinhold, F. *Chem. Rev.* **1988**, *88*, 899.
(49) Foster, J. P.; Weinhold, F. *J. Am. Chem. Soc.* **1980**, *102*, 7211.
(50) Weinhold, F.; Landis, C. R. *Valency and Bonding: A Natural Bond Orbital Donor-Acceptor Perspective*; Cambridge University Press: Cambridge, 2005.
(51) Momma, K.; Izumi, F. *J. Appl. Crystallogr.* **2011**, *44*, 1272.
(52) Dunnington, B. D.; Schmidt, J. R. *J. Chem. Theory Comput.* **2012**, *8*, 1902.
(53) Galeev, T. R.; Dunnington, B. D.; Schmidt, J. R.; Boldyrev, A. I. *Phys. Chem. Chem. Phys.* **2013**, *15*, 5022.
(54) Lee, C.; Wei, X.; Kysar, J. W.; Hone, J. *Science* **2008**, *321*, 385.
(55) Peng, Q.; Wen, X.; De, S. *RSC Adv.* **2013**, *3*, 13772.
(56) Liu, F.; Ming, P.; Li, J. *Phys. Rev. B* **2007**, *76*, 064120.
(57) Li, S. D.; Ren, G. M.; Miao, C. Q. *Inorg. Chem.* **2004**, *43*, 6331.
(58) Li, S.-D.; Miao, C.-Q.; Guo, J.-C.; Ren, G.-M. *J. Am. Chem. Soc.* **2004**, *126*, 16227.

DOI: 10.1021/ja513209c
J. Am. Chem. Soc. 2015, 137, 2757−2762